Journal of Physics: Conference Series **228** (2010) 012041 doi:10.1088/1742-6596/228/1/012041

ADC non-linear error corrections for low-noise temperature measurements in the LISA band

J Sanjuán[1,2], A Lobo[1,2], J Ramos-Castro[3], N Mateos[1] and M Díaz-Aguiló[4]

[1]Institut de Ciències de l'Espai, *CSIC*, Fac. de Ciències, Torre C5, 08193 Bellaterra, Spain
[2]Institut d'Estudis Espacials de Catalunya (*IEEC*), Gran Capità 2-4, 08034 Barcelona, Spain
[3]Dep. Eng. Electrònica, *UPC*, Campus Nord, Ed. C4, J Girona 1-3, 08034 Barcelona, Spain
[4]Dep. Física Aplicada, *UPC*, Campus Nord, Ed. B4/B5, J Girona 1-3, 08034 Barcelona, Spain

E-mail: sanjuan@ieec.fcr.es

Abstract. Temperature fluctuations degrade the performance of different subsystems in the *LISA* mission. For instance, they can exert stray forces on the test masses and thus hamper the required drag-free accuracy. Also, the interferometric system performance depends on the stability of the temperature in the optical elements. Therefore, monitoring the temperature in specific points of the *LISA* subsystems is required. These measurements will be useful to identify the sources of excess noise caused by temperature fluctuations. The required temperature stability is still to be defined, but a figure around $10\,\mu\mathrm{K\,Hz^{-1/2}}$ from 0.1 mHz to 0.1 Hz can be a good rough guess. The temperature measurement subsystem on board the *LISA* Pathfinder mission exhibits noise levels of $10\,\mu\mathrm{K\,Hz^{-1/2}}$ for f >0.1 mHz. For *LISA*, based on the above hypothesis, the measurement system should overcome limitations related to the analog-to-digital conversion stage which degrades the performance of the measurement when temperature drifts. Investigations on the mitigation of such noise will be here presented.

1. Introduction

LISA is a space-based gravitational wave detector with the primary scientific goal of observing *GW*s from astronomical sources in the frequency range from 0.1 mHz to 0.1 Hz [1]. However, the detection of *GW*s requires differential measurements of distance at the pico-meter level between two bodies separated by 5 million kilometres. This fact implies challenging requirements in the test masses' (*TM*s) residual acceleration noise in order to ensure *GW* detection with high signal-to-noise ratio. Otherwise *GW* signals will be buried in the random *TM*s motion associated to the forces acting on them. The *LISA* top level requirement, in terms of *TM* acceleration noise, is [2]

$$S^{1/2}_{\delta a,LISA}(\omega) \leq 3\times10^{-15}\cdot\left\{\left[1+\left(\frac{\omega/2\pi}{8\ \mathrm{mHz}}\right)^4\right]\left[1+\left(\frac{0.1\ \mathrm{mHz}}{\omega/2\pi}\right)\right]\right\}^{\frac{1}{2}}\ \mathrm{m\,s^{-2}\,Hz^{-1/2}} \qquad (1)$$

from 0.1 mHz to 0.1 Hz. One of the noise sources that can jeopardise the *LISA* performance is temperature fluctuations affecting key subsystems of the mission. More specifically, thermal stability is necessary to, first, ensure that the acceleration noise caused by temperature

fluctuations[1] in the *TM*s is kept below the top level requirement —see Eq. (1); and second, to ensure the stability of the optical elements properties of the interferometric systems[2] [3].

The very demanding requirements for the *LISA* mission led to recognise the need of a technology demonstration mission: the so-called *LISA* Pathfinder mission [4]. The main goal of *LPF* is to check if the residual acceleration in Eq. (1) can be achieved, i.e., it must verify the ability to set a *TM* in purely gravitational free fall to the level required by Eq. (1), although in *LPF* the requirements have been relaxed one order of magnitude below the *LISA* requirements both in amplitude and in frequency.

The *LISA* Technology Package[3] (*LTP*) includes a temperature measurement subsystem (*TMS*) in order to assess whether or not the required thermal stability is met, and to provide information of the actual coupling between temperature fluctuations and acceleration noise. At this moment the *LTP TMS* flight model version has been already designed and tested, and is compliant with the *LTP* requirements [5] —see Fig. 1. The *TMS* must exhibit noise levels of $10^{-5}\,\mathrm{K\,Hz^{-1/2}}$ from 1 mHz to 30 mHz in order to measure the expected temperature fluctuations in the *LTP*[4] with a good signal-to-noise ratio. However, such system exhibits *extra* noise in the submilli-Hertz range when the measured temperature drifts ($\sim \mu\mathrm{K\,s^{-1}}$). Although this is not a problem for the *LTP*, investigations are needed to overcome such limitation in view of *LISA*: the measurement bandwidth (*MBW*) stretches down to 0.1 mHz, the floor noise level requirement is one order of magnitude more demanding and, therefore, weaker temperature drifts can deteriorate the performance of the *TMS*.

The source of the excess noise has been seen to be due to non-idealities of the transfer curve of the analog-to-digital converter (*ADC*). A 16-bit successive approximation register (*SAR*) *ADC* is the only suitable option due to space qualification constraints. As shown in Fig. 1, the noise in the temperature measurement increases noticeably for $f < 0.1$ mHz when the measured temperature drifts are higher than $0.5\,\mu\mathrm{K\,s^{-1}}$. This paper focuses on the identification and mitigation of this problem. In Sec. 2 we review the theoretical basis of the noise introduced by a non-ideal *ADC*. In Sec. 3 we show how the effect of the *ADC* degrades the performance of *TMS* and how the theoretically expected noise and the experimental results agree. In Sec. 4 we describe a method to mitigate the noise coming from the *ADC*, the so-called *dithering techniques*. The test set-up and the experimental results using the dithering technique are shown in Sec. 5. Finally, Sec. 6 highlights the most relevant results.

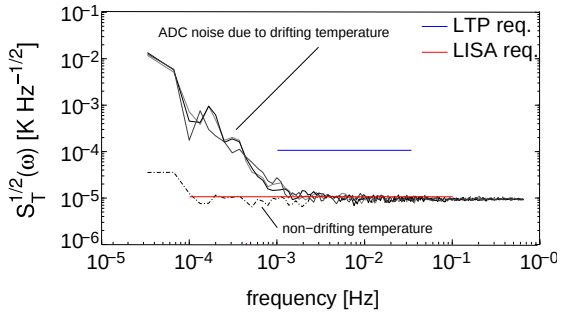

Figure 1. *LTP TMS* performance. The excess noise at low frequency (f <1 mHz) appears when the measured temperature drifts ("ADC noise due to drifting temperature" trace). It vanishes when the signal is kept constant ("non-drifting temperature" trace).

[1] Radiometer effect, radiation pressure or outgassing
[2] Changes of the index of refraction or dilatation (and contraction) cause an error in the acceleration measurement.
[3] The science module of the European Space Agency (*ESA*) in LPF.
[4] They are $10^{-4}\,\mathrm{K\,Hz^{-1/2}}$ from 1 mHz to 30 mHz.

2. Quantisation noise in *SAR ADC*s

In real *SAR ADC*s the quantisation steps are not uniform due to mismatches in their internal topology (tolerances in the capacitors, δC_k, of the *SAR* array). Such non-uniformity is specified with two parameters: differential non-linearity (*DNL*) and integral non-linearity (*INL*) [6]. The latter represents the difference between the real and the ideal *ADC* transfer curves. The noise introduced by this error is the one limiting the temperature measurement performance when drifting input signals are present. The voltage error ϵ_k[5] induced by an error in the k-th bit is:

$$\epsilon_k(v) \simeq \frac{b_k(v)\,\delta C_k}{(2^N-1)\,C}\,V_{\rm FS} = b_k(v)\,\frac{\delta C_k}{C}\,\Delta \qquad (k=0 \text{ is the } LSB) \tag{2}$$

where b_k is the binary digit (it is set to 0 or 1 depending on the sampled voltage), δC_k is $C_{k,\rm real} - 2^k C$, Δ ($\simeq V_{\rm FS}/2^N$) is the *ADC* quantisation step and N is the number of bits of the *ADC*. *LSB* stands for least significant bit. Equation (2) can be expressed as[6] [7]:

$$|\mathcal{Q}_k(\xi)| = \Delta \sum_{n=-\infty}^{\infty} \frac{\sin\frac{n\pi\epsilon_k}{2^{k+1}\Delta}}{n}\,\frac{\sin\frac{n\pi}{2}}{\sin\frac{n\pi}{2^{k+1}}}\,\delta\!\left(\xi - \frac{\pi n}{2^k\Delta}\right) \tag{3}$$

Equation (3) is graphically represented in Fig. 2 (center and bottom panels) where a superimposed periodic pattern in the quantisation error of the *ADC* with 1 *LSB* of amplitude and periodicity of $2^{k+1}\Delta$ (caused by the *INL* errors) is clearly seen.

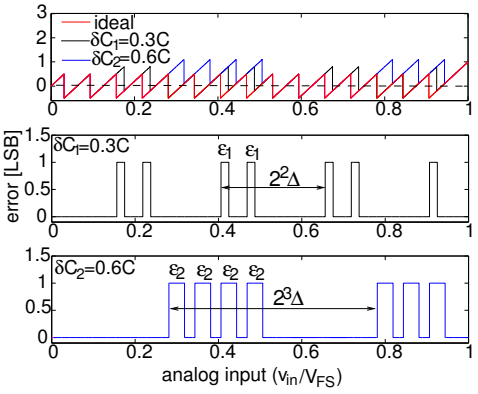

Figure 2. Top: quantisation error functions for an ideal *ADC* (red) and for two non-ideal *ADC*s with different error bits (black and blue). Centre and bottom: error differences between the non-ideal and ideal *ADC*s [$\epsilon_k(v)$].

3. Effect of *ADC* non-idealities on the *TMS*

To estimate *INL* induced errors in the temperature measurements let us assume the input signal is a straight line for a certain time interval:

$$v(t) = a + bt \quad \text{if} \quad 0 \le t \le t_{\rm max}, \ \text{otherwise } v(t) = 0 \tag{4}$$

[5] The difference between a real *ADC* (non-uniform quantisation steps) transfer curve and an ideal *ADC* (uniform quantisation steps) transfer curve.

[6] We have defined the Fourier transform in the voltage domain by $\mathcal{Q}(\xi) \equiv \int_{-\infty}^{\infty} q(v)e^{-i\xi v}dv$. Not to be mistaken by the usual time/frequency Fourier transforms. We use special symbols for this to avoid confusion. ξ is the Fourier-conjugate variable of v, and is accordingly measured in 2π volts^{-1}.

In this case, Eq. (3) becomes (in the frequency, 2π Hz, domain)[7] [8]:

$$|\tilde{q}_k(\omega)| = \Delta \sum_{n=-\infty}^{\infty} \frac{\sin\frac{n\pi\epsilon_k}{2^{k+1}\Delta}}{n} \frac{\sin\frac{n\pi}{2}}{\sin\frac{n\pi}{2^{k+1}}} \delta\left(\omega - \frac{\pi n|b|}{2^k\Delta}\right) \tag{5}$$

and the main frequency component introduced by an error in the k-th bit is located at[8]:

$$\omega_{1_k} = \frac{\pi 2^N}{2^k V_{\rm FS}} |\dot{v}(t)| \ , \quad \dot{\omega}_{1_k} = \frac{\pi 2^N}{2^k V_{\rm FS}} |\ddot{v}(t)| \tag{6}$$

From Eqs. (6) some conclusion can be drawn:

- high-slope signals at the *ADC* input translate into high-frequency components at the output of the *ADC*,
- errors in the higher bits show up as noise at lower frequency than errors in the lower bits,
- consequently, high-slope inputs combined with errors in high bits may show up as excess noise in the bandwidth of interest,
- the fundamental frequency associated to a bit error varies with variations of $\dot{v}(t)$, hence the error in the bit spreads across the frequency band when $\ddot{v}(t) \neq 0$.

Figure 3 shows experimental data and the theoretical expected evolution of the power spectrum density with time —cf. Eq. (6). They are in excellent agreement.

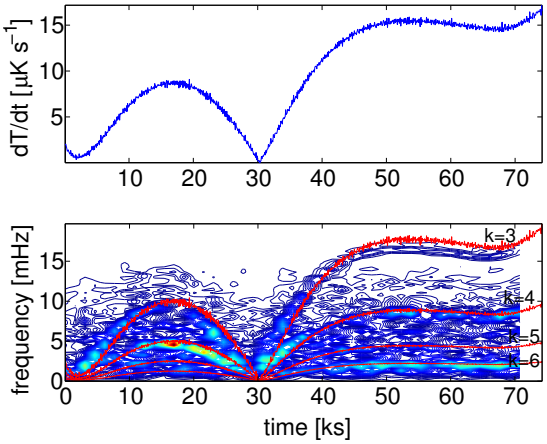

Figure 3. Top: absolute value of the input signal slope, $|\dot{v}(t)|$, of a temperature measurement run. The sensitivity at the input of the *ADC* is $\simeq$1.35 V K^{-1}, hence, temperature drifts vary between 0 and 9.3 μK s^{-1}. Bottom: spectrogram of the top panel measurement. The energy of the signal is concentrated in specific frequencies which change with time precisely following $|\dot{v}(t)|$, as predicted by Eq. (6), and as shown in red dashed traces labelled by the order of the corresponding bit error (in this case from $k = 3$ to $k = 6$).

[7] Dirac δ-functions are the result of infinite length integration intervals in Fourier transform calculations. In any practical situation the δ-functions remain sinc-functions.

[8] These expressions are valid when the temperature signals can be conveniently approximated by a series of concatenated ramps with adequate slopes and lengths.

4. Mitigation of non-ideal *ADC* errors: dithering techniques

Two different methods have been used to mitigate the effect of the non-idealities of the *ADC*s on the temperature measurements. Both methods are based on the same technique: *dithering signals*. This technique is based on the injection of suitable analog signals to the signal of interest before quantisation in order to *linearise* the *ADC* transfer curve. In the following we briefly review the theoretical basis of this technique. If a dither voltage, d, with a certain probability density function (*PDF*), $p(d)$, is added (before quantisation) to the signal of interest, v, the average quantisation error at the output of the *ADC* is [9]:

$$\langle q(v)\rangle = \int_{-\infty}^{\infty} q(v+z)\,p(z)\,dz \tag{7}$$

$$\langle \mathcal{Q}(\xi)\rangle = \mathcal{Q}(\xi)\,\mathcal{P}^*(\xi) \tag{8}$$

where $q(v)$ [and $Q(\xi)$] is the quantization error of a real *ADC* —see Sec. 2—, $p(d)$ is the *PDF* of the dither signal [and $P(\xi)$ is the Fourier transform as defined in footnote 6)] and $\langle q(v)\rangle$ [and $\langle Q(\xi)\rangle$] is the quantisation error function at the output of the *ADC* considering we inject a dither signal. In our experiments we have tested two different dither signals: (i) Gaussian noise dither added out of the *MBW* and (ii) triangular wave dither of frequency 50 Hz. These signals are characterised by the following equations:

$$\text{Gaussian noise}: \quad p(d) = \frac{1}{(2\pi)^{1/2}\sigma}\,e^{-\frac{d^2}{2\sigma^2}} \rightarrow \mathcal{P}(\xi) = e^{-\sigma^2\xi^2/2} \tag{9}$$

$$\text{Triangular wave}: \quad p(d) = \frac{1}{D} \qquad \rightarrow \qquad \mathcal{P}(\xi) = \text{sinc}(D/2)\xi \tag{10}$$

where σ and D are the standard deviation of the Gaussian noise and the amplitude of the triangular wave, respectively; and $\xi = \frac{2\pi}{2^{k+1}\Delta}$. Figure 4 shows the error components introduced by error bits (k=0 and k=3) and the effect of the dither signals on them (red traces).

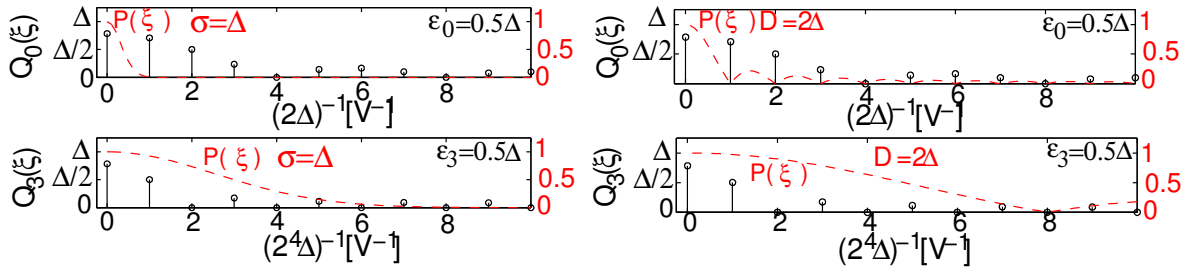

Figure 4. *ADC* quantisation error as given in Eq. (3). They are indicated by the circles on top of vertical strokes. Left: the red dashed line represents the Gaussian dither attenuation profile with $\sigma = \Delta$ which suffices to mitigate the error in the bit $k = 0$ but not the errors in $k = 3$. To do so higher values of σ are required. Right: *idem* for the triangular wave dither of amplitude $D = 2\Delta$. Note the different scales in the x-axis. The conversion to Hertz is easily done by using $\xi = \omega/|\dot{v}(t)|$.

5. Test set-up and results

The test set-up in order to check the performance of the dithering methods implemented consisted in attaching a set of thermistors inside a thermal insulator designed to screen out temperature fluctuations to the required level in the milli-Hertz range, i.e., $< 10^{-5}\,\text{K}\,\text{Hz}^{-1/2}$ at

the milli-Hertz [3]. A temperature control was implemented to generate temperature ramps of different slopes (from $0.5\,\mu\mathrm{K\,s^{-1}}$ to $16\,\mu\mathrm{K\,s^{-1}}$) inside the insulator. In this manner we could observe the effect of the dither signals in the *TMS* under different temperature slopes.

Four configurations were tested under identical conditions. First, a 16-bit *SAR ADC* (AD977 of Analog Devices[9]) without any dither signal was tested. Second, we tested the same *ADC* but injecting Gaussian noise dither before quantisation. The third configuration consisted in using the triangular wave dither signal. Finally, a higher resolution 24-bit Delta-Sigma *ADC*[10] was also used for comparison. Results are shown in Fig. 5 for different slopes and configurations.

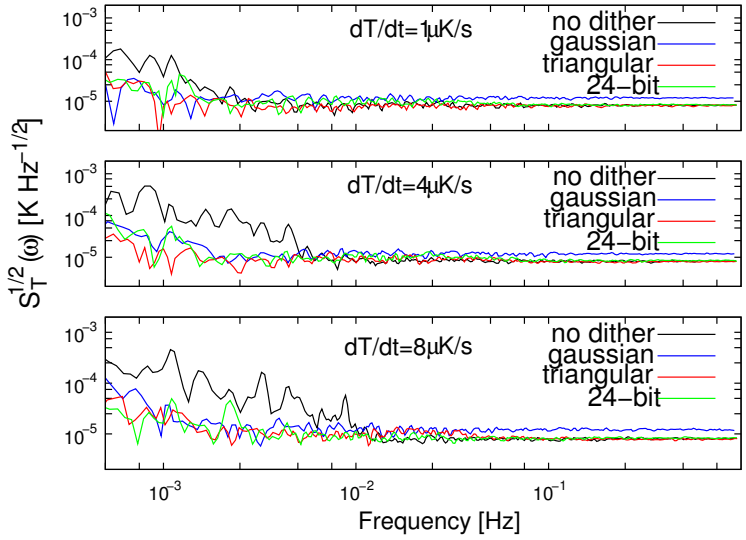

Figure 5. Linear Spectral Density for different configurations. As can be seen in absence of dither, the noise of the *ADC* increases (in amplitude and bandwidth) with the slope of the input signal. Gaussian noise dither attenuates this effect although the floor noise is slightly higher than the typical one. Triangular wave dither works satisfactorily and the floor noise remains untouched. The 24-bit Delta-Sigma *ADC* works also well for the tested slopes.

6. Conclusions

The analysis and results obtained lead to the following conclusions:

- Extra noise caused by *INL* errors of the *ADC* was seen at the lower end of the *LTP MBW* when drifting temperatures were measured with the *LTP* temperature measurement subsystem.
- For temperature slopes $>0.5\,\mu\mathrm{K\,s^{-1}}$ the extra noise challenges the performance of the *LTP* measuring system[11], the problem growing more severe at lower frequencies (*LISA* band).
- The use of dithering techniques mitigates the *INL* errors introduced by the *ADC*. However the injection of Gaussian noise dither increases the floor noise of the system in the *MBW*. Alternatively, the triangular wave dither does not add noise in the *MBW* and, therefore, results in a more efficient attenuation of *INL* errors. Dither technique is not foreseen to fly in *LPF*, but the results obtained herein are important in view of designing a more robust

[9] The *ADC* used for the space model is the Texas Instruments ADS7809 which is based in the same structure.
[10] Such *ADC* should exhibit less non-linearity problems. Space qualified version of these *ADC*s are not available.
[11] The expected slopes in the *LTP* (in nominal conditions) are lower than $0.5\,\mu\mathrm{K\,s^{-1}}$.

TMS for the *LISA* mission. The dither signal to be injected in the system will depend on the expected temperature drifts in *LISA* and, apparently, the triangular dither signal should be able to cope with the requirements of the mission. This would avoid the use of 24-bit Delta-Sigma *ADCs* which they are not suitable for multiplexed systems as in the case of the *TMS* and, furthermore, at present they are not space qualified.

Acknowledgments

Support for this work came from Project ESP2004-01647 of Plan Nacional del Espacio of the Spanish Ministry of Science and Innovation (MICINN). JS acknowledges a grant from MICINN.

References

[1] Bender P *et al.* 2000 ESA Report No ESA-SCI(2000)11
[2] The LISA International Science Team 2008 ESA-NASA Report No LISA-ScRD-Iss5-Rev1
[3] Lobo A, Nofrarias M, Ramos-Castro J and Sanjuán J 2006 *Class Quantum Grav* **23** 5177
[4] Vitale S *et al* 2005 Science Requirements and Top-level Architecture Definition for the LISA Technology Package (*LTP*) on Board *LISA* Pathfinder (SMART-2), report no. LTPA-UTN-ScRD-Iss003-Rev1
[5] Sanjuán J, Lobo A, Nofrarias M, Ramos-Castro J and Riu P 2007 *Rev Sci Instr* **78** 104904
[6] Hoeschele DF 1994 *Analog-to-digital and digital-to-analog conversion techniques* (New York, NY: Wiley)
[7] Wagdy MF 1996 *IEEE Trans Instrum Meas* **45** 610
[8] Sanjuán J 2009 *Development and validation of the thermal diagnostics instrumentation in LISA Pathfinder* PhD dissertation
[9] Wagdy MF 1989 *IEEE Trans Instrum Meas* **38** 850